# *Kapd* Is Essential for Specification of the Dopaminergic Neurogenesis in Zebrafish Embryos

Jangham Jung[1], Eunhee Kim[2], and Myungchull Rhee[1,2,]*

[1]Department of Life Science, BK21 Plus Program, Graduate School, Chungnam National University, Daejeon 34134, Korea,
[2]Department of Biological Sciences, College of Bioscience and Biotechnology, Chungnam National University, Daejeon 34134, Korea
*Correspondence: mrhee@cnu.ac.kr
https://doi.org/10.14348/molcells.2021.0005
www.molcells.org

To define novel networks of Parkinson's disease (PD) pathogenesis, the substantia nigra pars compacta of A53T mice, where a death-promoting protein, FAS-associated factor 1 was ectopically expressed for 2 weeks in the 2-, 4-, 6-, and 8-month-old mice, and was subjected to transcriptomic analysis. Compendia of expression profiles and a hierarchical clustering heat map of differentially expressed genes associated with PD were bioinformatically generated. Transcripts level of a particular gene was fluctuated by 20, 60, and 0.75 fold in the 4-, 6-, and 8-month-old mice compared to the 2 months old. Because the gene contained Kelch domain, it was named as *Kapd* (Kelch-containing protein associated with PD). Biological functions of *Kapd* were systematically investigated in the zebrafish embryos. First, transcripts of a zebrafish homologue of *Kapd*, *kapd* were found in the floor plate of the neural tube at 10 h post fertilization (hpf), and restricted to the tegmentum, hypothalamus, and cerebellum at 24 hpf. Second, knockdown of *kapd* caused developmental defects of DA progenitors in the midbrain neural keel and midbrain–hindbrain boundary at 10 hpf. Third, overexpression of *kapd* increased transcripts level of the dopaminergic immature neuron marker, *shha* in the prethalamus at 16.5 hpf. Finally, developmental consequences of *kapd* knockdown reduced transcripts level of the markers for the immature and mature DA neurons, *nkx2.2, olig2, otx2b,* and *th* in the ventral diencephalon of the midbrain at 18 hpf. It is thus most probable that Kapd play a key role in the specification of the DA neuronal precursors in zebrafish embryos.

**Keywords:** FAF1, Kapd (Kelch-containing protein associated with PD), midbrain dopaminergic neurons, next-generation sequencing, Parkinson's disease

## INTRODUCTION

Progressive loss of dopaminergic (DA) neurons in the substantia nigra pars compacta (SNpc) is the leading cause of Parkinson's disease (PD) (Fearnley and Lees, 1991; Hassler, 1938). Neuronal loss in the nigral complex occurs over the course of normal aging, as well as in neurodegenerative disease. Pathogenic clues to PD suggest that the regional selectivity of the lesions is specific to the neuropathological progression of PD and is therefore related to the molecular networks underlying prodromal PD. In sporadic PD, the most widespread form of parkinsonism, Lewy body pathology is associated with synucleinopathy. Sporadic PD is linked to protein misfolding and the development of abnormal intracellular inclusions. The presence of these aggregates is essential for neuropathologic confirmation of the clinical diagnosis (Giasson et al., 2000; Tofaris and Spillantini, 2007). Although the majority of PD is sporadic, familial forms of parkinsonism also exist; these cases are associated with genetic defects in factors such as LRRK2, α-synuclein, UCH-L1, DJ-1, ATP13A2, Parkin, and PINK1 (Klein and Westenberger, 2012). The syndrome also develops as a

sequel to intoxication, trauma, vascular alterations, and metabolic diseases implicated in the formation and degradation of α-synuclein (α-Syn) aggregates (Forno, 1969; Galvin et al., 2001; Wakabayashi et al. 2007). Fas-associated factor 1 (FAF1), identified as a death-promoting protein (Ryu et al., 1999), participates in Fas-induced apoptosis as a member of the death-inducing signaling complex, and in regulated necrosis through activation of poly (ADP-ribose) polymerase 1 (PARP1). In addition, FAF1 contributes to cell death in dopaminergic neurons through PARP1 activation following oxidative stress (Sul et al., 2013; Yu et al., 2016). Hence, it would be worthwhile to discover the molecular networks that connect FAF1 with PD pathogenesis.

To elucidate the molecular elements composing SNpc region where FAF1 contributes to PD pathogenesis, we used A53T mice, a model of PD. In A53T mice, the 53th residue of α-Syn is mutated from alanine to threonine, resulting in a pathologic hallmark of PD: formation of Lewy bodies, neuronal inclusions consisting largely of α-Syn aggregations (Golbe et al., 1990; Polymeropoulos et al., 1996; 1997). Using A53T mice from 2 to 8 months of age, we generated transcriptomic profiles of the SNpc in the presence or absence of FAF1. This approach provided a broader dynamic range as well as high specificity and sensitivity for the unbiased detection of key genes and transcripts. Based on the transcriptomic data, we generated profiles of differential gene expression corresponding to the stages of neurodegenerative pathogenesis. The profiles, generated from total RNA isolated from the SNpc of mice at 2, 4, 6, and 8 months of age, were subjected to sequential bioinformatics analysis with ExDEGA, STRING-db, DAVID, KEGG Mapper, GSEA-MSigDB, and MeV to identify differentially expressed genes associated with PD (DEG-PDs). Among these genes, we focused on *DEG-13* because its transcript levels in the right hemisphere of mice ectopically expressing FAF1 increased by 20- and 60-fold at 4 and 6 months, respectively, relative to 2 months. *DEG-13* encodes a member of the KLHDC family (Dhanoa et al., 2013) that contains one Kelch repeat motif and 3 & 4 Kelch domains at the N-terminus. Hence, we designated DEG-13 as Kapd (Kelch-containing protein associated with PD).

Prior to investigating Kapd as a cause of PD, we studied the biological functions of *kapd* in zebrafish, a species that completes the entire process of embryogenesis with 3 days. Here, we report the spatiotemporal expression patterns and putative functions of *kapd* based on the developmental consequences of its knockdown and ectopic expression in the brain. In addition, we discuss networks that are likely to connect *kapd* with PD pathogenesis.

## MATERIALS AND METHODS

### Mouse model of PD
This study was approved by the Institutional Animal Care and Use Committee in Chungnam National University (approval No. CNU-00920). All the mice were maintained in the animal facility of Chungnam National University (Daejeon, Korea), and all animal studies were conducted in accordance with the institutional guidelines for the care and use of laboratory animals. The mice were randomly assigned to either MPTP or

saline-treated groups. To generate the FAF1-induced mouse model of PD, the viral vector of FAF1 (4.3 × 10$^{13}$ GC/ml) was injected into the right hemisphere of TG mice. The mice were killed 14 days after the last injection, and the brains were processed for further analysis. The A53T mice were kindly provided by Professor Eunhee Kim (Department of Bioscience & Biotechnology, Graduate School, Chungnam National University, Daejeon, Korea).

### Stereological virus injection
Stereotaxic adeno-associated virus (AAV) injections were performed as described by Kim (Sul et al., 2013) with some modifications. In brief, the AAV type 1 expressing FAF1 (AAV1-FAF1) was purchased from Vector Biolabs (USA). For stereotaxic injection of AAV1-FAF1 into the substantia nigra of the mouse midbrain, male A53T at 2, 4, 6, and 8 months after birth mice were anesthetized with an intraperitoneal injection of a mixture of Zoletil 50 (Virbac, USA) and Rompun (Bayer Korea, Korea). A 33 gauge injection needle was used to stereotaxically inject AAV1-FAF1 into the right substantia nigra (anteroposterior, 3.0 mm; mediolateral, 1.2 mm; dorsoventral, 4.3 mm from bregma). The infusion into the substantia nigra was performed at a rate of 0.1 μl/min, and 1.25 μl of AAV1-FAF1 (4.3 × 10$^{13}$ GC/ml) was injected. After the injection, the needle was left in the substantia nigra for an additional 5 min and then slowly withdrawn. The skin over the injection site was closed by suturing. The AAV1-FAF1 was kindly provided by Professor Eunhee Kim (Department of Bioscience & Biotechnology, Graduate School, Chungnam National University, Daejeon, Korea).

### RNA isolation
Total RNA was isolated using Trizol reagent (Invitrogen, USA). RNA quality was assessed by Agilent 2100 bioanalyzer using the RNA 6000 Nano Chip (Agilent Technologies, The Netherlands), and RNA quantification was performed using ND-2000 Spectrophotometer (Thermo Fisher Scientific, USA).

### Library preparation and sequencing
Libraries were prepared from total RNA using the NEBNext Ultra II Directional RNA-Seq Kit (New England BioLabs, UK). The isolation of mRNA was performed using the Poly(A) RNA Selection Kit (Lexogen, Austria). The isolated mRNAs were used for the cDNA synthesis and shearing, following manufacture's instruction. Indexing was performed using the Illumina indexes 1-12. The enrichment step was carried out using of polymerase chain reaction (PCR). Subsequently, libraries were checked using the Agilent 2100 bioanalyzer (DNA High Sensitivity Kit) to evaluate the mean fragment size. Quantification was performed using the library quantification kit using a StepOne Real-Time PCR System (Life Technologies, USA). High-throughput sequencing was performed as paired-end 100 sequencing using Hiseq X10 (Illumina, USA).

### RNA-Seq data analysis
mRNA-Seq reads were mapped using TopHat software (Trapnell et al., 2009) tool in order to obtain the alignment file. The alignment files also were used for assembling transcripts,

estimating their abundances and detecting differential expression of genes, isoforms using cufflinks. We used the FPKM (fragments per kilobase of exon per million fragments) as the method of determining the expression level of the gene regions. The FPKM data were normalized based on Quantile normalization method using EdgeR within R (R Development Core Team, 2016). Data mining and graphic visualization were performed using ExDEGA (Ebiogen, Korea). GO annotation enrichment was performed using DAVID (Sherman et al., 2009) with default parameters. KEGG pathway analysis was conducted using KEGG Mapper (Kanehisa and Sato, 2020). Gene clustering was performed using MeV ver. 4.9.0. Protein network analysis was performed using String Apps of Cytoscape ver. 3.7.2.

### Zebrafish care and embryos
Wild-type (WT) zebrafish was obtained from Korea Zebrafish Organogenesis Mutant Bank (ZOMB) and grown at 28.5°C. Embryos were obtained through natural spawning and raised, and staged as described previously (Jung et al., 2020). Embryonic pigmentation was blocked by treating the embryos with 0.002% phenylthiourea after onset of somitogenesis.

### Morpholino, *in vitro* transcription, and microinjections
Splicing-blocking morpholino (I2/E3: 5′ACGCACACACCT-GCAAAGGA GGAGGAGAG-3′) and five-base mismatch morpholino (5-mismatch MO) were purchased from Gene-Tools (USA), and dissolved in water. *kapd*_specific mor-

pholinos (0.2 to 1 ng) or control morpholinos were injected into zebrafish embryos at the 1-cell stage. *kapd* mRNA was synthesized using the Ambion mMESSAGE mMACHINE kit according to the manufacturer's instructions. mRNAs were dissolved in nuclease-free water and diluted in 0.5% phenol red solution for microinjection via a Picopump microinjection device (WPI, USA).

### Whole-mount *in situ* hybridization (WISH)
Embryos were fixed in 4% paraformaldehyde (PFA) overnight, and dehydrated in 100% methanol. Embryos after 24 h post-fertilization (hpf) were digested with 10 μg/ml protease K (Thermo Fisher Scientific). WISH was performed with minor modifications as described in Jung et al. (2020). Antisense probes of *kapd* were synthesized from a specific region within the ORF. Antisense probes of *kapd* were synthesized using the DIG RNA Labeling Kit (T7) (Roche, USA).

### Statistical analysis
All data were presented as mean ± SD. Statistically significant differences between the two groups were determined using the two-tailed Student's *t*-test. Statistical significance was calculated using one-way ANOVA with multiple comparisons between groups analyzed by Dunnett's test. Statistical analysis was performed using SPSS Statistics (ver. 17.0; SPSS, USA), and $P$ value < 0.05 was considered statistically significant.
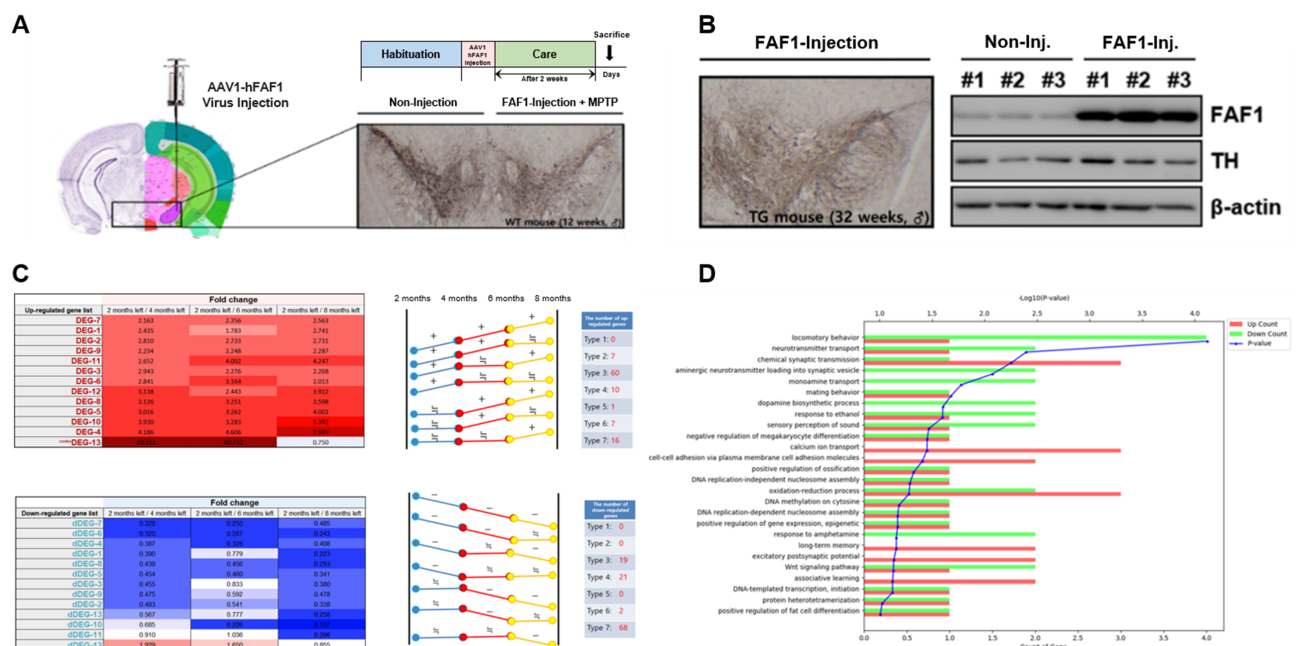


**Fig. 1.** Transcriptomic analysis of dopaminergic neurons in 2- to 8-month-old A53T transgenic mice in the presence or absence of FAF1. (A) Stereotaxic injection of a viral vector expressing FAF1. FAF1 viral vector (4.3 × 10^{13} genome copies [GC]/ml) was injected into the right hemisphere of TG mice. (B) Striatal and midbrain sections of 4 to 6 mice per group were immunostained using an affinity-purified polyclonal antibody against tyrosine hydroxylase (TH). Relative changes in the expression of specific proteins were analyzed on the samples (25 μg of protein per lane). Inj., injection. (C) DEGs with significant fold changes confirmed the purity of isolated dopaminergic neurons. (D) Top 35 DAVID functional annotation categories for *Mus musculus* gene IDs. The numbers of genes assigned to the top 26 functional categories obtained from DAVID GO chart analysis are shown for up- and downregulated genes (red and green, respectively).

## RESULTS

### SNpc-specific transcriptional profiles and gene regulatory networks identify DEG-13 as Kapd (Kelch-containing protein associated with PD)

To separate and identify SNpc DA neuronal populations in A53T mice at 2, 4, 6, and 8 months of age, we injected a viral vector expressing FAF1 into the midbrain of the right hemisphere. After 2 weeks, we immunostained for tyrosine hydroxylase (TH), a marker of mature DA neurons which is an entry enzyme into dopamine synthesis and FAF1 in midbrain sections from each group using affinity-purified polyclonal antibodies against TH and FAF1, respectively (Figs. 1A and 1B). FAF1 was expressed at higher levels in the right hemisphere (FAF1-injected side) than in the left hemisphere, whereas TH was detected within the normal range (Fig. 1B). To identify DEGs associated with the pathogenesis of PD in the presence and absence of FAF1, total RNA from the SNpc of A53T and WT mice was subjected to next-generation sequencing (NGS). A total of 23,284 genes were screened and plotted for each sample (Supplementary Fig. S1). In the figure, red denotes up-regulation at a particular position, whereas blue denotes down-regulation. DA neuron markers in the adult SNpc (Allen Brain Atlas, ABA), including *Slc6a3* (*Dat*), *Fam184a*, *Ankrd34b*, *Nwd2*, and *Cadps2*, confirmed that FAF1 was localized in mDA SNpc labeled with the markers TH and DAT (Supplementary Fig. S2).

To determine whether these DEGs modulate functions of key transcriptional regulators in PD-associated pathways, we subjected validated DEGs to pathway and functional category enrichment analysis using the Kyoto Encyclopedia of Genes and Genomes (KEGG) and the Database for Annotation, Visualization and Integrated Discovery (DAVID) (Fig. 1D). Categorization of DEGs by KEGG pathway analysis revealed that the top three gene annotations were 'extracellular matrix', 'aging', and 'inflammatory response' (data not shown). The functional analysis revealed that the upregulated DEGs were significantly enriched for the terms 'chemical synaptic transmission' and 'oxidation-reduction process', whereas downregulated DEGs were significantly enriched in 'locomotory behavior', 'neurotransmitter transport', and 'dopamine biosynthetic process' (Fig. 1D). Genes specifically expressed in the SNpc DA neuron clusters by dissection of neuroanatomical domain and further revealing regional subclusters based on iterative marker genes analyses might correlate their preferential vulnerability to PD pathogenesis. These analyses identified *DEG-13* as an upregulated SNpc-specific gene. Using ExDEGA, we converted principal components into quantile normalized expression estimates of mRNAs in each sample.

Principal component analysis identified *DEG-13* as an upregulated DEG according to the following criteria: fold change in
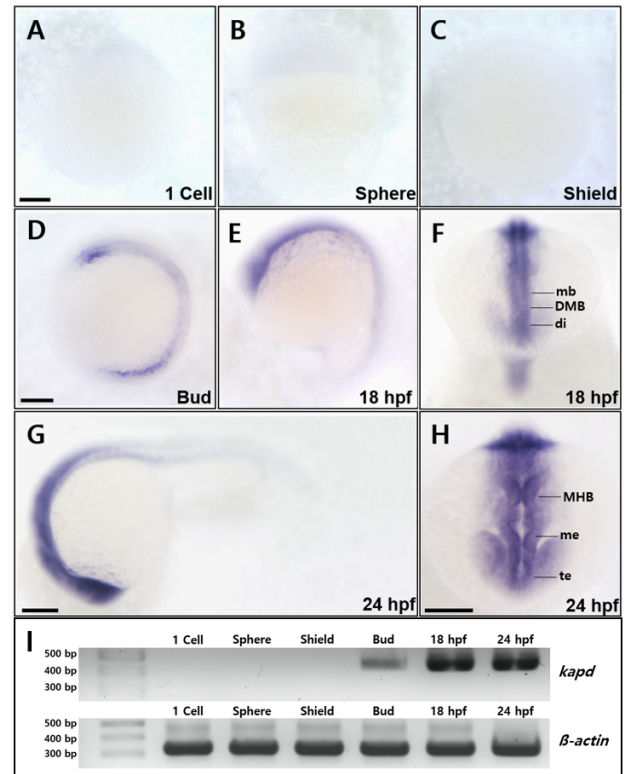


**Fig. 2. Spatiotemporal expression patterns of zebrafish *kapd*.** WISH analysis of *kapd* from the one-cell stage through 36 hpf. (A-C) Transcripts of *kapd* were not detected from the one-cell stage through the shield stage. (D) At the bud stage, *kapd* transcripts were first detected in the FP cell of the neural tube. (E and F) Transcripts were abundant in the central nervous system from 10 hpf through to 18 hpf. At 18 hpf, *kapd* transcripts were distributed in the precursor region of the midbrain, including the diencephalic-mesencephalic boundary along the anterior-posterior (AP) axis (F). (G and H) At 24 hpf, *kapd* expression was restricted to the forebrain through the hindbrain including the telencephalon, mesencephalon, and rhombomere (H). (I) RT-PCR analysis of *kapd* transcripts at the developmental stages in zebrafish embryos. *β-actin* was used as loading control. (A-H) Scale bars = 250 μm. All embryos were collected synchronously from WT zebrafish for WISH analysis at the corresponding stages. mb, midbrain; DMB, diencephalic-mesencephalic boundary; di, diencephalon; MHB, midbrain-hindbrain boundary; me, mesencephalon; te, telencephalon.

**Table 1.** mRNA profiles of *Kapd* in the FAF1-enriched SNpc of A53T mice

| DEG-13 (NM_178253) | 2 mo/L | 2 mo/R | 4 mo/L | 4 mo/R | 6 mo/L | 6 mo/R | 8 mo/L | 8 mo/R |
|---|---|---|---|---|---|---|---|---|
| | Non | FAF1 | Non | FAF1 | Non | FAF1 | Non | FAF1 |
| Raw data | 215 | 212 | 5180 | 359 | 10563 | 2753 | 280 | 202 |
| Normalized RC (log$_2$) | 7.908 | 7.838 | 12.252 | 7.930 | 13.832 | 12.071 | 8.014 | 7.566 |

Data visualization was done based on the UCSC genome browser for the mouse assembly mm10, $P < 0.05$.
mo, month; L, left; R, right; RC, read count.

expression (FC) ≥ 2 (i.e., log$_2$(FC) ≥ 1) and $P < 0.05$. Among the DEGs whose expression was affected by induction of FAF1, *DEG-13* was highly upregulated (Supplementary Fig. S2). The pattern of *DEG-13* changed over the lifespan: at 4 and 6 months relative to 2 months of age, the gene was upregulated by 20- and 60-fold, respectively. By contrast, at 8 months relative to 6 months, the gene was downregulated 60-fold (Fig. 1C). In other words, DEG-13 was validated among the DEGs as a gene significantly downregulated in the FAF1-injected hemisphere from 2 to 8 months of age in comparison to the control (Table 1).

Neighborhood correlation (http://www.neighborhood-correlation.org) compares sequence similarity, alignment length, and domain architecture comparison by classifying single and multidomain homologs with high accuracy. A rank plot showed that DEG-13 contains significant matches to the human F-box protein 42 gene (*FBXO42*) in the curated database. Mutations in the F-box protein 7 gene (*FBXO7*) cause Parkinsonian-pyramidal syndrome, an autosomal recessive form of Parkinsonism (Di Fonzo et al., 2009). *FBXO42*, a paralog of *FBXO7*, encodes a protein involved in the ubiquitin–proteasome system that may play a role in the pathogenesis of PD (Gao et al., 2013). *DEG-13*, a paralog of *FBXO42*, is involved in the Cul5-type ubiquitin–proteasome-mediated

degradation of the selenoprotein SELENOS (Okumura et al., 2020). As shown in Supplementary Fig. S3E, DEG-13 contains one Kelch repeat motif and two 3 & 4 Kelch domains at the N-terminus, whereas the zebrafish homolog encodes 4 & 5 Kelch domains and one F-Box–associated motif; this information was obtained from the Conserved Domain Database by the National Center for Biotechnology Information (NCBI). Based on these findings, DEG-13 was named as Kapd.

## Knockdown of *kapd* causes developmental defects in the midbrain during neurulation

We used zebrafish to investigate the functions of *kapd* because of its advantages as an experimental model (Laale, 1977). First, we visualized the spatiotemporal expression patterns of *kapd* in zebrafish embryos using WISH. *kapd* transcripts appeared at the bud stage in the floor plate (FP) at the primordium of the anterior central nervous system and the posterior trunk of the neural tube (Fig. 2D). At 18 hpf, *kapd* transcripts were localized predominantly in the forebrain, midbrain, and hindbrain along a clear midline (Figs. 2E and 2F), and expanded to the cranial neural crest at 24 hpf (Figs. 2G and 2H). The neural FP in the anterior regions of in zebrafish embryos rolls up and fuses dorsally to directly generate the central canal, giving rise to tel-, mes-, and di-en-
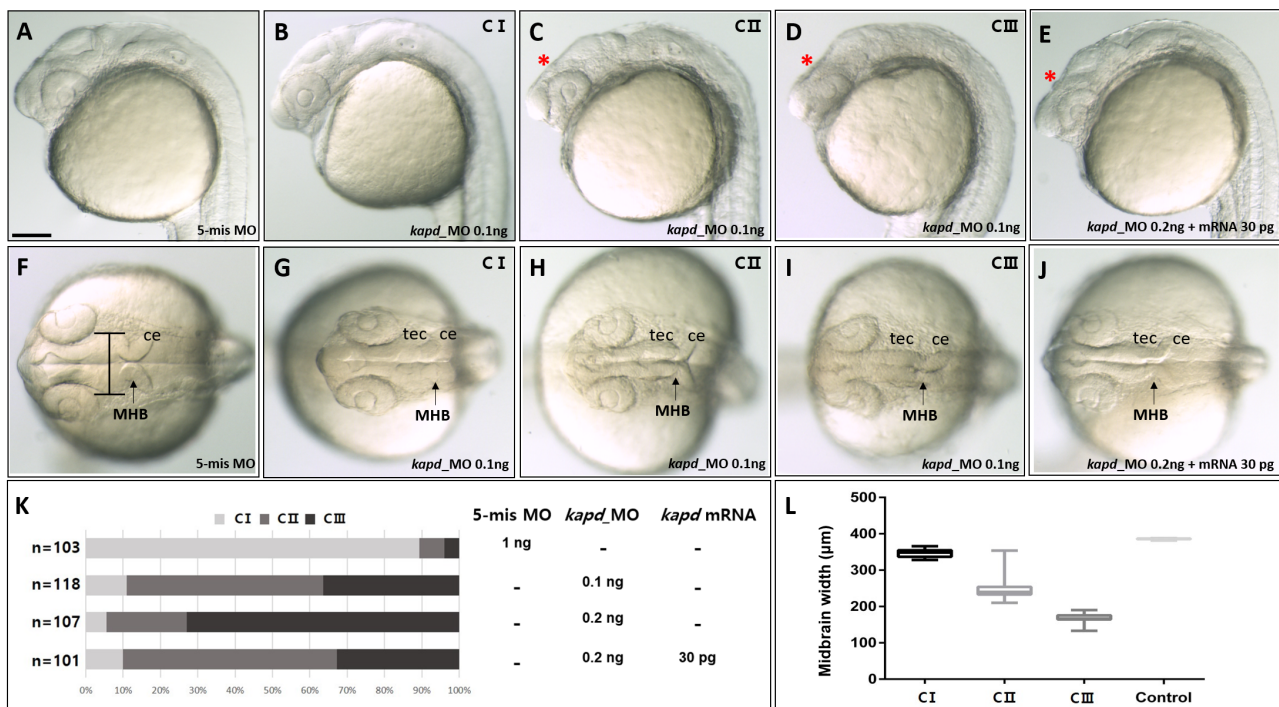


**Fig. 3. Repression of *kapd* expression decreases the size of the mesencephalon, including the midbrain ventricle, at 24 hpf.** Microinjection of *kapd* morpholino (0.1 ng) into an embryo at the one-cell stage to knock down DEG-13. (A) 5-mismatch MO and (B-D) *kapd* morphants were categorized as class I, II, or III (C I, C II, or C III). (E) Rescue of a *kapd* morphant (0.2 ng) with *kapd* mRNA (30 pg). (F-J) Dorsal view of the midbrain, midbrain-hindbrain boundary, and hindbrain of *kapd* morphants at 24 hpf. (F) 5-mismatch MO. (G-I) At 24 hpf, embryos were injected with *kapd* MO. (J) *kapd* mRNA (30 pg) was injected into a *kapd* morphant at the one-cell stage (0.2 ng). (K) The proportion of moderately deformed embryos (class II) was higher after rescue with *kapd* mRNA. (L) Measurement of midbrain widths revealed a significant reduction of the neural tube in *kapd* morphants. Statistical significance was calculated using one-way ANOVA, and multiple comparisons between groups were analyzed by Dunnett's test. (A-J) Scale bar = 250 μm. MHB, midbrain-hindbrain boundary; ce, cerebellum; tec, tectum.

cephalon (Clarke, 2009). Therefore, we investigated whether *kapd* contributes to the process of neurulation in zebrafish embryogenesis.

To assess the role of *kapd* in neurulation, we employed antisense morpholinos to knock down its expression. Microinjection of *kapd*-specific antisense oligonucleotide morpholinos (*kapd* MOs; 0.1 ng per embryo) into zebrafish embryos at the one-cell stage caused significant reduction of the midbrain, including the midbrain ventricle, at 24 hpf (Figs.

3D and 3F). Morphological defects were categorized into three classes on the basis of severity: class I (Fig. 3B), without distinguishable defects; class II (Fig. 3C), reduced midbrain volume, shrunken neural tube, and ventricle contraction; and class III (Fig. 3D), shortened head and no discernible neural tube. *kapd* MOs generated class II and class III embryos in a dose-dependent manner (Fig. 3K). At doses of 0.1 and 0.2 ng per embryo, *kapd* MOs generated class III at rates of 38% and 72%, respectively. To quantitate morphological defects
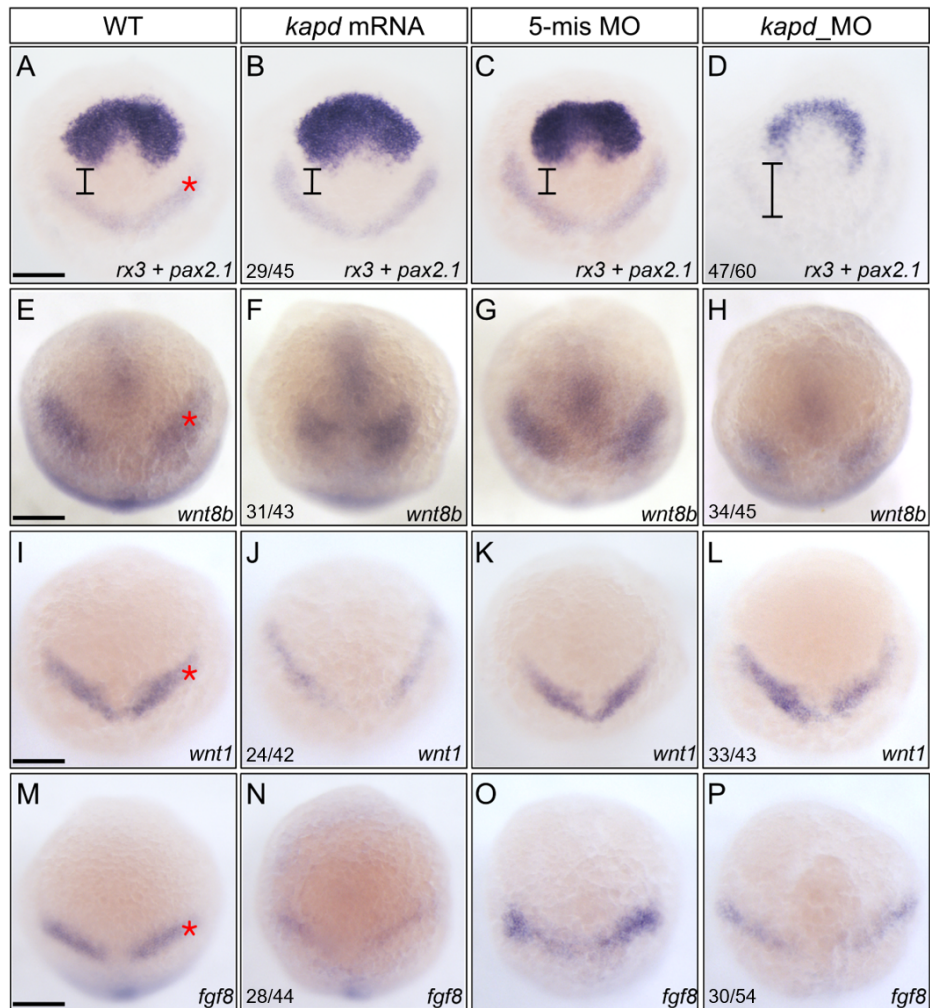


**Fig. 4. Spatiotemporal expression patterns of markers for presumptive midbrain and DA progenitors at 10 hpf.** (A-D) WISH analysis using *rx3* and *pax2.1* as a molecular marker for the forebrain and midbrain domains indicates that loss of *kapd* function disrupted the presumptive midbrain development. (A) WT embryo. Microinjection of *kapd* mRNA (30 pg per embryo) into wild-type embryos thickened the anterior forebrain (B). *kapd* 5-mismatch control embryos had the similar expression patterns in the presumptive midbrain (C) to that of WT (A). In contrast, knock-down of *kapd* (0.2 ng morpholino per embryo) repressed MHB (asterisk) and telencephalic precursors in *kapd* morphants at 10 hpf (D). (E-H) WISH analysis with *wnt8b* as a molecular marker for the midbrain in anterior brain patterning. *wnt8b* transcripts were present in the midbrain of WT (E) and control embryos injected with 5-mismatch (G). Overexpression of *kapd* (*kapd* mRNA 30 pg per embryo) shortened the MHB area (F) while knock-down of *kapd* (0.2 ng of *kapd* morpholino per embryo) remarkably reduced the level of *wnt8b* transcripts in the MHB (asterisk) and anterior midbrain of the morphants (H). (I-P) WISH analysis with *wnt1* and *fgf8* as molecular markers for DA progenitors at 10 hpf. WT embryos (I and M), embryos injected with *kapd* mRNA (J and N). *kapd* mRNA injected embryos showed narrower and reduced expression patterns for *wnt1* (J) and *fgf8* (N). The level of *wnt1* transcripts was not significantly changed in the midbrain neural keel region of *kapd* morphants (L). However, transcripts of *fgf8* were reduced in the MHB neural keel in comparison to those of control embryos at 10 hpf (M-P). (A-P) Scale bars = 250 μm.

in neurulation of *kapd* morphants, we measured the width of the midbrain at 24 hpf, and then performed imaging and statistical analysis (Fig. 3L). *kapd* morphants all had reduced midbrain size. When *kapd* was ectopically expressed via microinjection of *kapd* mRNA (30 pg per embryo) into *kapd* morphants (0.2 ng per embryo) at the one-cell stage, the morphological defects in the midbrain and neural tube were significantly rescued, and wild-type phenotypes were restored (Figs. 3E and 3J). Neural crest cells are continuously produced at the lateral edges of the neural plate, suggesting that neural crest-promoting signals are present for the initial induction of neurulation (Moury and Jacobson, 1990). Together, these observations indicate that proper expression of *kapd* is essential for the development of the midbrain during the neurulation period.

### *kapd* modulates differentiation of DA progenitor cells in the presumptive midbrain

The positional specification of the dopaminergic cell lineage during normal development is regulated by extrinsic factors that impose regional characteristics on DA progenitors at early developmental stages (Holzschuh et al., 2003). To elucidate the requirement for *kapd* in specification of pre-sumptive midbrain, we injected *kapd* morpholino (0.1 ng) or mRNA (50 pg per embryo) into wild-type zebrafish embryos at the one-cell stage. *kapd* morphants and embryos over-expressing *kapd* were subjected to WISH analysis using the markers *rx3* and *pax2.1* for forebrain and MHB (midbrain–hindbrain boundary), respectively (Stigloher et al., 2006). In embryos overexpressing *kapd*, the expression patterns of *rx3* and *pax2.1* in the presumptive midbrain at 10 hpf were similar to those in controls (Figs. 4A-4C; square brackets). By contrast, knockdown of *kapd* altered the transcript levels of both *rx3* and *pax2.1* from the rostral MHB to the telencephalon region without eye field at 10 hpf (Figs. 4C and 4D). The expression patterns of Wnts, BMPs (bone morphogenetic proteins) and FGFs (fibroblast growth factors), which are markers of the neural crest derivatives and DA progenitors, were examined following overexpression and knockdown of *kapd* at 10 hpf (Arenas, 2014; Liem et al., 1995; Nguyen et al., 1998; Villanueva et al., 2002). Wnt8, which is involved in neural crest induction and differentiation of DA neurons, is expressed at the diencephalic anlage in the midbrain, hypothalamus, and MHB at 24 hpf (Duncan et al., 2015; Lewis et al., 2004; Russek-Blum et al., 2008). Transcripts levels of *wnt8b* were remarkably reduced in the midbrain neural keel
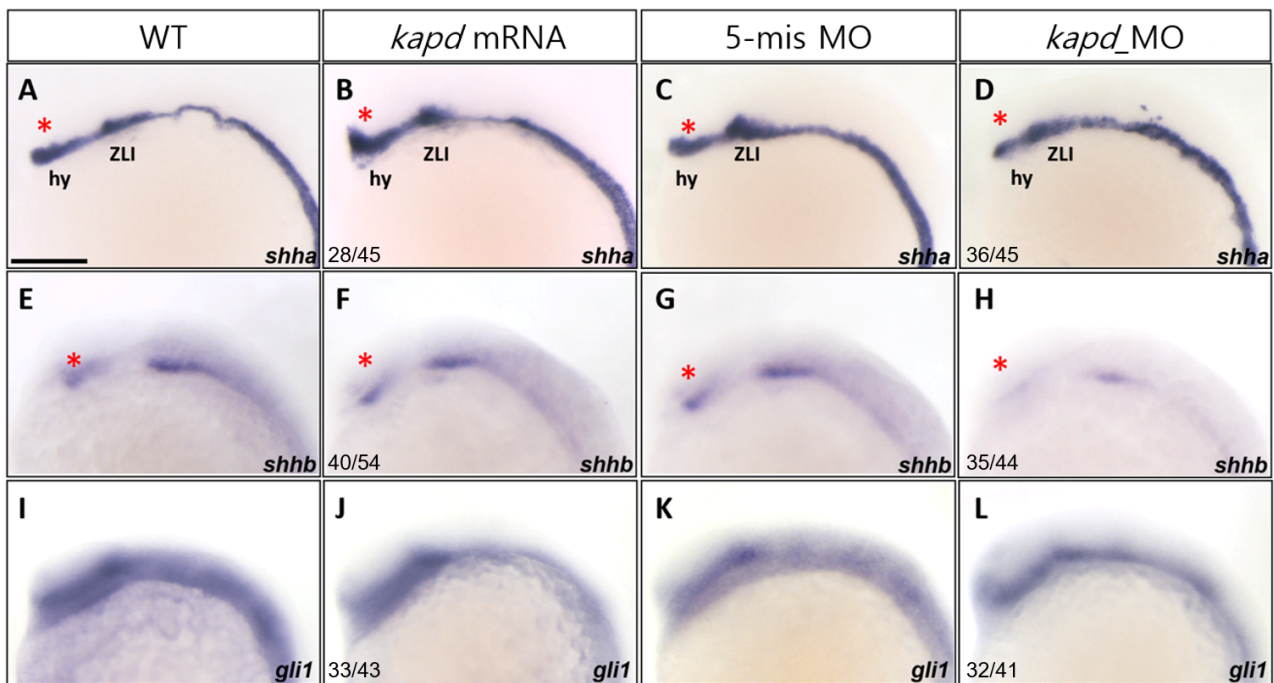


Fig. 5. Knockdown of *kapd* expression alters the expression patterns of the molecular markers *shha* and *shhb*. (A-D) WISH analysis using *shha* as a molecular marker for the thalamus (asterisks) and zona limitans intrathalamica (ZLI) revealed that loss of *kapd* function disrupts diencephalic differentiation. (A) WT embryo. Microinjection of *kapd* mRNA (50 pg per embryo) into WT embryos increased expression in the hypothalamus (hy) (B). Expression patterns of *kapd* in the hypothalamus of 5-mismatch MO control embryos (C) were similar to those of WT embryos (A). By contrast, in *kapd* morphants at 16.5 hpf, knockdown of *kapd* (0.2 ng MO per embryo) decreased expression in the hypothalamus (D). (E-H) *shhb* transcripts were present in the ventral FP (asterisks) of WT embryos at 16.5 hpf (E). Overexpression of *kapd* did not cause significant changes in the ventral FP of the forebrain (F), whereas knockdown of *kapd* (0.2 ng of *kapd* morpholino per embryo) markedly decreased the level of *shhb* transcripts in the ventral diencephalon of the morphants (H). Embryos were examined for expression of the ventral neural marker, *gli1*, at 16.5 hpf. Transcript levels of *gli1* were not affected by overexpression or knockdown of *kapd* (I-L). (A-L) Scale bar = 250 μm.

in the morphants, accompanying shrinkage of the MHB neural plate, but were not altered significantly in WT or controls at 10 hpf (Figs. 4E-4H). Expression patterns of *wnt1* in *kapd* morphants were similar to those in WT and 5-mismatch control embryos (Figs. 4I-4L). On the other hand, overexpression of *kapd* dramatically decreased expression of *wnt1* (Fig. 4J). Transcript levels of *dkk1b*, an antagonist of Wnt and a neural tube marker (Glinka et al., 1998), were robustly elevated in the prechordal plate region, significantly elevating the number of dopaminergic neurons at 18 hpf, relative to the 5-mismatch MO control (data not shown). Hence, it is conceivable that *kapd* contributes to development of the midbrain neural keel and MHB, as well as to specification of DA precursors, via networks involving Wnts and FGFs.

## *kapd* contributes to SHH signaling involved in the mDA neuronal differentiation

As neurulation continues, neural ectoderm cells produce a pseudostratified epithelium, undergoing polarized cell divisions to establish a well-defined midline by 18 hpf (Ciruna et al., 2006; Clarke, 2009). In cranial neurulation and neural crest migration, laterally segregated cells are apparent by 12 hpf, and convergence movements form the neural keel by 14 hpf, the neural rod at 18 hpf (when the clear midline is established), and finally the neural tube at 20 hpf. The development of diencephalic DA cells in the hypothalamus, ventral thalamus and caudal diencephalon may contribute to specification of DA cell lineage (Smeets and Reiner, 1994). To determine how *kapd* is involved in the differentiation of dopaminergic neurons, we analyzed the expression patterns of *shha* and *shhb*, which are markers of the FP and notochord (Ertzer et al., 2007), respectively, upon ectopic expression or knockdown of *kapd*. Overexpression of *kapd* expanded the expression domain of *shha* from the ventral toward the dorsal hypothalamus in the midbrain (Fig. 5B), which is closely involved in the specification of mesodiencephalic dopaminergic (mdDA) neurons (Mesman et al., 2014). Knockdown of *kapd* substantially decreased the expression area of *shha* in the zona limitans intrathalamica (ZLI) and hypothalamus (Fig. 5D). Knockdown of *kapd* abolished the domain of *shhb* transcripts in the ventral diencephalic area of the FP (Fig. 5H). Gli1 is an activator of SHH target genes, whereas Gli1 activity is transcriptionally not required for initial SHH signaling (Bai et al., 2002). To investigate the possible role of *kapd* in SHH signaling, we assayed the expression patterns of *gli1* upon ectopic expression or knockdown of *kapd*. Interestingly, the expression patterns of *gli1* at 16.5 hpf were not significantly altered by overexpression or knockdown of *kapd* (Figs. 5I-5L). These observations confirm that *kapd* contributes to SHH signaling, lending further support to the idea that SHH and *kapd* regulate development of both the FP and midbrain organizer (Hegarty et al., 2013) in the ventral diencephalon.

## *kapd* is required for differentiation of the DA precursor cells to the DA neurons

To investigate the molecular mechanism by which knockdown of *kapd* changes the regulatory networks associated with differentiation of the immature DA neurons, we visualized spatiotemporal expression of markers of immature DA neurons of the ventral diencephalon, *nkx2.2* and *olig2*, in *kapd* morphants at 18 hpf (Borodovsky et al., 2009; Briscoe et al., 1999). The SHH-responsive gene *nkx2.2* is a type II homeodomain transcriptional regulator required for specification of ventral cell populations (Briscoe et al., 1999); it is expressed in Otp-dependent DA neurons at the medial hypothalamus (Del Giacco et al., 2008). The level of *nkx2.2* transcripts was markedly decreased in the ventral diencephalon, including the hindbrain ventral region, in *kapd* morphants relative to WT and control embryos at 18 hpf (Figs. 6B and 6C).

In zebrafish, *olig2* is expressed in a SHH signal-dependent manner in a subset of diencephalic progenitors committed to a DA neuronal fate (Barth and Wilson, 1995; Guner and Karlstrom, 2007; Park et al., 2002). Expression of *olig2* begins in the ventral neural tube before *nkx2.2* and is extinguished prior to terminal DA differentiation (Al Oustah et al., 2014). To determine whether knockdown of *kapd* affects development of the ventral diencephalon, we analyzed the expression patterns of *olig2* in *kapd* morphants at 18 hpf. The domain expressing *olig2* was significantly diminished in *kapd* morphants relative to WT and control embryos (Figs. 6D-6F). Therefore, it is likely that proper expression of *kapd* is essential for differentiation of DA precursors into immature DA neurons in the ventral diencephalon and dorsal forebrain at 18 hpf. Consequently, expression of *th,* a marker of mature DA neurons in the ventral diencephalon (Filippi et al., 2010), completely disappeared in DA neurons of *kapd* morphants (Figs. 6G-6I).

To determine whether *kapd* plays roles in regulating both DA neurons and late midbrain neural crest cells, we examined the expression of markers of the DA lineage. Otx2b, a marker of the midbrain, is normally expressed in DA progenitors and mature DA neurons in the ventral midbrain (Simeone et al., 2011). Zic2b, a marker of the cranial neural crest, influences induction of neural crest at the neural plate border (TeSlaa et al., 2013). WISH analysis revealed that *otx2b* expression was reduced in the midbrain and forebrain ventricle of *kapd* morphants relative to WT and 5-mismatch MO control embryos (Figs. 6G-6I). Knockdown of *kapd* specifically repressed expression of *zic2b* in the neural crest of the midbrain region in *kapd* morphants (Fig. 6O) relative to control embryos (Figs. 6M and 6N) at 18 hpf. Therefore, it is likely that *kapd* is essential for cranial neural crest induction and midbrain neural tube morphogenesis, which are prerequisites for development of DA precursors and specification of DA neurons.

## DISCUSSION

### Identification of *DEG-13* at the prodromal phase of PD in the transcriptomic files

Some genes critical to PD age of onset, rather than risk, have been identified; however, loci that modulate risk have been discovered much more successfully than those that modulate age of onset. A genome-wide study revealed that *DEG-13* influences age of onset in both familial and non-familial PD (Hill-Burns et al., 2016). Consistent with these data, in this study we identified core transcriptional factors implicated in PD pathogenesis, based on the genetic architecture of familial and non-familial PD, using FAF1-induced A53T mice. Tran-
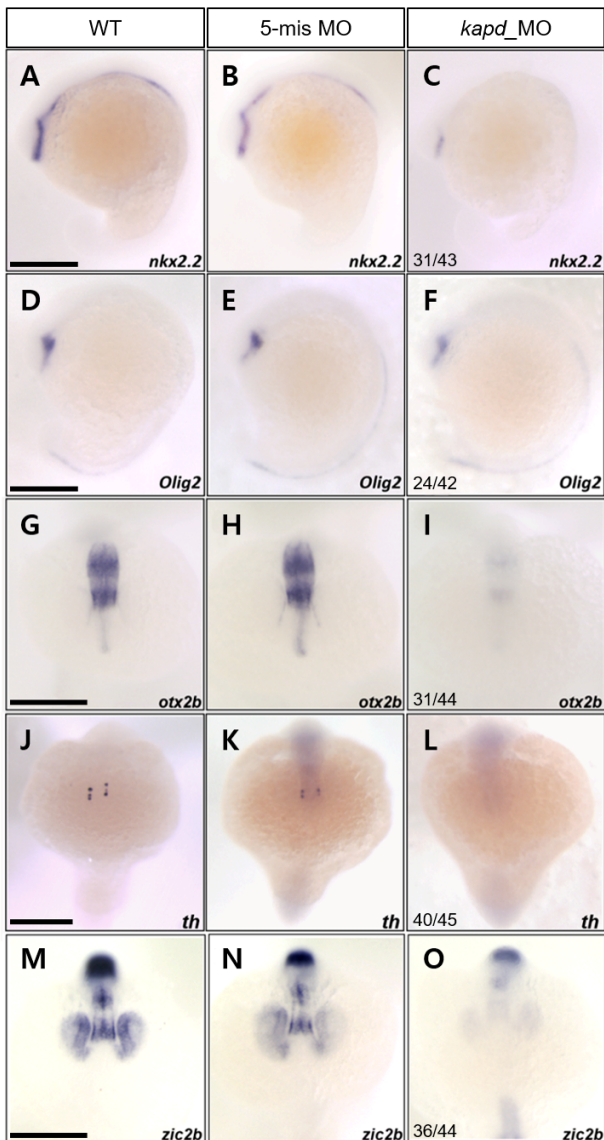
Fig. 6. Knockdown of *kapd* decreases the transcript levels of markers of immature and mature DA neurons in the ventral diencephalon at 18 hpf. (A-F) WISH analysis with *nkx2.2*- and *olig2*-specific probes detected reduction in their transcripts in the ventral diencephalon at 18 hpf. (A) WT embryo, (B) 5-mismatch MO control, and (C) *kapd* MO (0.2 ng of *kapd* morpholino per embryo). (G-L) WISH analysis of *kapd* MO (0.2 ng of *kapd* morpholino per embryo) using *otx2b* and *th* as probes. (G) *otx2b* transcripts in the midbrain of WT embryos at 18 hpf. (H) Embryos injected with 5-mismatch showed similar patterns to those of WT embryos. (I) *kapd* MO shows remarkable reduction of *otx2b* transcripts in the midbrain including midbrain ventricle at 18 hpf. Transcripts of *th* in WT (J), 5-mismatch control (K), and *kapd* MO (L) at 18 hpf. *th* transcripts were present in the ventral diencephalon in WT and 5-mismatch control whereas the expression was lost in the corresponding areas of *kapd* morphants. (M-O) Embryos were examined for the expression of neural crest marker, *zic2b* at 18 hpf. Transcripts of *zic2b* in WT (M) and 5-mis MO control (N). Injection of *kapd* MO caused notable reduced *zic2b* expression domains, ventral diencephalic and mesencephalic region at 18 hpf (O). (A-O) Scale bars = 100 μm.

scriptomic profiling revealed that *Kapd* (*Klhdc1*) was up-regulated 20- and 60-fold in 4- and 6-month-old mice, respectively, relative to 2-month-old mice, whereas expression was dramatically reduced at 8 months, reflecting dramatic motor impairment and premature lethality. Our study also corroborates the results of segregation analyses that discovered DEGs with critical effects on age of onset of familial PD during the prodromal period. The data presented here highlight the advantages of our approach and the qualified performance compared with databases of PD patients.

## Positional specification of the dopaminergic cell lineage under normal expression of *kapd*

According to the Conserved Domain Database administered by the NCBI, mouse Kapd contains one Kelch repeat motif and two 3 & 4 Kelch domains at the N-terminus, whereas zebrafish *kapd* encodes 4 & 5 Kelch domains and one F-Box–associated motif. Kelch repeat proteins play important roles in a variety of human neurological disorders such as GAN (giant axonal neuropathy) and brain tumors (Bomont et al., 2000). Other Kelch repeat proteins participate in physiological processes including cell signaling, protein trafficking, and transcriptional regulation (Chin et al., 2007).

We demonstrated that *kapd* expression in the midbrain is required for induction and maintenance of *nkx2.2* and *olig2* in the prethalamus, as well as for induction of *th* in the diencephalic anlage (Fig. 6). All of these are pro-neural genes involved in SHH signaling-driven neurogenesis of neural progenitor cells and specification of DA neuronal identities in the midbrain (Jessell, 2000). Ubiquitin-dependent regulation of translation is an important feature of cell fate determination. For example, the ubiquitin ligase CUL3 in complex with its vertebrate-specific substrate adaptor KBTBD8 (Kelch repeat and BTB domain-containing protein 8) is an essential regulator of human neural crest specification (Werner et al., 2015). Our description of the maturation of the diencephalic DA neurons serves as a further example of this. Thus, SHH signaling is essential for the involvement of *kapd* in neural crest specification in the midbrain and subsequent generation of DA neuronal identities.

Interestingly, *kapd* morphants exhibited no significant change in *pitx3* expression patterns at 18 hpf, whereas knockdown of *kapd* decreased expression of *nurr1* relative to the controls (Supplementary Fig. S4). Because Pitx3 potentiates Nurr1 in specification of the dopaminergic phenotype in mice (Jacobs et al., 2009), it is very likely that *kapd* modulates Nurr1-mediated transcription in mdDA neurons. This, in turn, implies that Pitx3 is a crucial factor for the specification of the dopaminergic phenotype. In regard to the proposed modulatory effect of FAF1 in this PD mouse model, our data provide evidence that the pathogenic transcription factor, *kapd* is an essential regulator of the DA cell lineage.

## Establishment of diencephalic anlage based on *kapd* and SHH signaling

Knockdown of *kapd* substantially decreased the area of *shha* expression in the ZLI and prethalamus. By contrast, overexpression of *kapd* increased the expression domain of the hypothalamus in the diencephalic anlage (Fig. 5B). To confirm
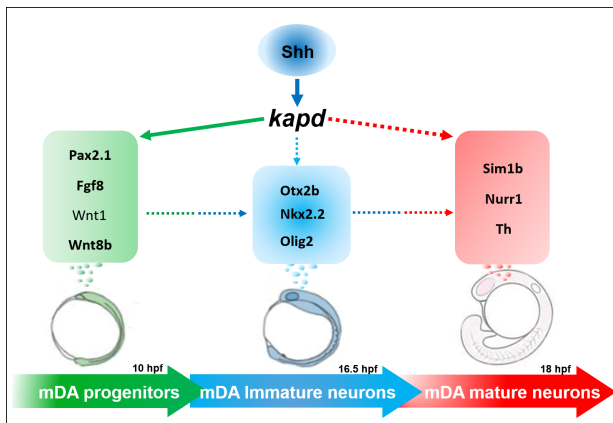
**Fig. 7. *kapd* is associated with genetic networks controlling the development of mDA neurons in zebrafish system.** The diagram summarizes the sequential stages and the molecules involved in the mDA neuron embryonic development. The expression of *kapd* is involved in cranial neural crest induction and midbrain neural tube morphogenesis, which are prerequisites for differentiation and maturation of the mDA neurons at various embryonic stages. Lines depict possible interactions among these molecules and arrows indicate stimulatory effects. The green colored, delimited by a green box, molecules involved in mDA progenitors. The light blue colored groups in box and circle are involved in immature mDA neurons. The red colored area clusters the genes involved in mature mDA identity.

loss of function, we administered the SHH inhibitor cyclopamine to embryos ectopically expressing *kapd* from 4 hpf until the time of sacrifice. The spatiotemporal expression patterns of *shha* at 16.5 hpf revealed that overexpression of *kapd* did not rescue the *shha* expression domain in the prethalamus (n = 35/44; data not shown). By contrast, knockdown of *kapd* caused severe phenotypic changes, including shortening of the spinal cord and delayed brain patterning (data not shown). Taken together with the data from our SHH inhibitor studies, these observations imply that *kapd* acts downstream of SHH signaling (Fig. 7) to play a critical role in the formation of the prethalamus.

*Note: Supplementary information is available on the Molecules and Cells website (www.molcells.org).*

## AUTHOR CONTRIBUTIONS
M.R. conceived and supervised the study. E.K. provided FAF1 and A53T model system which are critical to the study platform. J.J. performed the experiments and analyzed the data. J.J. and M.R. wrote and revised the manuscript.

## CONFLICT OF INTEREST
The authors have no potential conflicts of interest to disclose.

## ORCID
Jangham Jung      https://orcid.org/0000-0003-2806-3698
Eunhee Kim        https://orcid.org/0000-0002-7738-1222
Myungchull Rhee   https://orcid.org/0000-0002-4595-7573

## REFERENCES

Al Oustah, A., Danesin, C., Khouri-Farah, N., Farreny, M.A., Escalas, N., Cochard, P., Glise, B., and Soula, C. (2014). Dynamics of sonic hedgehog signaling in the ventral spinal cord are controlled by intrinsic changes in source cells requiring sulfatase 1. Development *141*, 1392-1403.

Arenas, E. (2014). Wnt signaling in midbrain dopaminergic neuron development and regenerative medicine for Parkinson's disease. J. Mol. Cell Biol. *6*, 42-53.

Bai, C.B., Auerbach, W., Lee, J.S., Stephen, D., and Joyner, A.L. (2002). Gli2, but not Gli1, is required for initial Shh signaling and ectopic activation of the Shh pathway. Development *129*, 4753-4761.

Barth, K.A. and Wilson, S.W. (1995). Expression of zebrafish nk2.2 is influenced by sonic hedgehog/vertebrate hedgehog-1 and demarcates a zone of neuronal differentiation in the embryonic forebrain. Development *121*, 1755-1768.

Bomont, P., Cavalier, L., Blondeau, F., Hamida, C.B., Belal, S., Tazir, M., Demir, E., Topaloglu, H., Korinthenberg, R., Landrieu, P., et al. (2000). The gene encoding gigaxonin, a new member of the cytoskeletal BTB/kelch repeat family, is mutated in giant axonal neuropathy. Nat. Genet. *26*, 370-374.

Borodovsky, N., Ponomaryov, T., Frenkel, S., and Levkowitz, G. (2009). Neural protein Olig2 acts upstream of the transcriptional regulator Sim1 to specify diencephalic dopaminergic neurons. Dev. Dyn. *238*, 826-834.

Briscoe, J., Sussel, L., Serup, P., Hartigan-O'Connor, D., Jessell, T.M., Rubenstein, J.L.R., and Ericson, J. (1999). Homeobox gene Nkx2.2 and specification of neuronal identity by graded Sonic hedgehog signalling. Nature *398*, 622-627.

Chin, K.T., Xu, H.T., Ching, Y.P., and Jin, D.Y. (2007). Differential subcellular localization and activity of kelch repeat proteins KLHDC1 and KLHDC2. Mol. Cell. Biochem. *296*, 109-119.

Ciruna, B., Jenny, A., Lee, D., Mlodzik, M., and Schier, A.F. (2006). Planar cell polarity signalling couples cell division and morphogenesis during neurulation. Nature *439*, 220-224.

Clarke, J. (2009). Role of polarized cell divisions in zebrafish neural tube formation. Curr. Opin. Neurobiol. *19*, 134-138.

Del Giacco, L., Pistocchi, A., Cotelli, F., Fortunato, A.E., and Sordino, P. (2008). A peek inside the neurosecretory brain through Orthopedia lenses. Dev. Dyn. *237*, 2295-2303.

Dhanoa, B.S., Cogliati, T., Satish, A.G., Bruford, E.A., and Friedman, J.S. (2013). Update on the Kelch-like (KLHL) gene family. Hum. Genomics *7*, 1-7.

Di Fonzo, A., Dekker, M.C.J., Montagna, P., Baruzzi, A., Yonova, E.H., Guedes, L.C., Szczerbinska, A., Zhao, T., DubbelHulsman, L.O.M., de Graaff, E., et al. (2009). FBXO7 mutations cause autosomal recessive, early-onset parkinsonian-pyramidal syndrome. Neurology *72*, 240-245.

Duncan, R.N., Panahi, S., Piotrowski, T., and Dorsky, R.I. (2015). Identification of Wnt genes expressed in neural progenitor zones during zebrafish brain development. PLoS One *10*, e0145810.

Ertzer, R., Müller, F., Hadzhiev, Y., Rathnam, S., Fischer, N., Rastegar, S., and Strähle, U. (2007). Cooperation of sonic hedgehog enhancers in midline expression. Dev. Biol. *301*, 578-589.

Fearnley, J.M. and Lees, A.J. (1991). Ageing and Parkinson's disease: substantia nigra regional selectivity. Brain *114*, 2283-2301.

Filippi, A., Mahler, J., Schweitzer, J., and Driever, W. (2010). Expression of the paralogous tyrosine hydroxylase encoding genes th1 and th2 reveals the full complement of dopaminergic and noradrenergic neurons in zebrafish larval and juvenile brain. J. Comp. Neurol. *518*, 423-438.

Forno, L.S. (1969). Concentric hyalin intraneuronal inclusions of Lewy type in the brains of elderly persons (50 incidental cases): relationship to parkinsonism. J. Am. Geriatr. Soc. *17*, 557-575.

Galvin, J.E., Lee, V.M.Y., and Trojanowski, J.Q. (2001). Synucleinopathies: clinical and pathological implications. Arch. Neurol. *58*, 186-190.

Gao, K., Deng, X., Zheng, W., Song, Z., Zhu, A., Xiu, X., and Deng, H. (2013). Genetic analysis of the FBXO42 gene in Chinese Han patients with Parkinson's disease. BMC Neurol. *13*, 125.

Giasson, B.I., Jakes, R., Goedert, M., Duda, J.E., Leight, S., Trojanowski, J.Q., and Lee, V.M. (2000). A panel of epitope-specific antibodies detects protein domains distributed throughout human α-synuclein in lewy bodies of Parkinson's disease. J. Neurosci. Res. *59*, 528-533.

Glinka, A., Wu, W., Delius, H., Monaghan, A.P., Blumenstock, C., and Niehrs, C. (1998). Dickkopf-1 is a member of a new family of secreted proteins and functions in head induction. Nature *391*, 357-362.

Golbe, L.I., Di Iorio, G., Bonavita, V., Miller, D.C., and Duvoisin, R.C. (1990). A large kindred with autosomal dominant Parkinson's disease. Ann. Neurol. *27*, 276-282.

Guner, B. and Karlstrom, R.O. (2007). Cloning of zebrafish nkx6. 2 and a comprehensive analysis of the conserved transcriptional response to Hedgehog/Gli signaling in the zebrafish neural tube. Gene Expr. Patterns *7*, 596-605.

Hassler, R. (1938). Zur Pathologie der Paralysis agitans und des postenzephalitischen Parkinsonismus. J. Psychol. Neurol. *48*, 387-476. German.

Hegarty, S.V., Sullivan, A.M., and O'keeffe, G.W. (2013). Midbrain dopaminergic neurons: a review of the molecular circuitry that regulates their development. Dev. Biol. *379*, 123-138.

Hill-Burns, E.M., Ross, O.A., Wissemann, W.T., Soto-Ortolaza, A.I., Zareparsi, S., Siuda, J., Lynch, T., Wszolek, Z.K., Silburn, P.A., Ritz, B., et al. (2016). Identification of genetic modifiers of age-at-onset for familial Parkinson's disease. Hum. Mol. Genet. *25*, 3849-3862.

Holzschuh, J., Hauptmann, G., and Driever, W. (2003). Genetic analysis of the roles of Hh, FGF8, and nodal signaling during catecholaminergic system development in the zebrafish brain. J. Neurosci. *23*, 5507-5519.

Jacobs, F.M., van Erp, S., van der Linden, A.J., von Oerthel, L., Burbach, J.P.H., and Smidt, M.P. (2009). Pitx3 potentiates Nurr1 in dopamine neuron terminal differentiation through release of SMRT-mediated repression. Development *136*, 531-540.

Jessell, T.M. (2000). Neuronal specification in the spinal cord: inductive signals and transcriptional codes. Nat. Rev. Genet. *1*, 20-29.

Jung, J., Choi, I., Ro, H., Huh, T.L., Choe, J., and Rhee, M. (2020). march5 Governs the convergence and extension movement for organization of the telencephalon and diencephalon in zebrafish embryos. Mol. Cells *43*, 76.

Kanehisa, M. and Sato, Y. (2020). KEGG Mapper for inferring cellular functions from protein sequences. Protein Sci. *29*, 28-35.

Klein, C. and Westenberger, A. (2012). Genetics of Parkinson's disease. Cold Spring Harb. Perspect. Med. *2*, a008888.

Laale, H.W. (1977). The biology and use of zebrafish, Brachydanio rerio in fisheries research. A literature review. J. Fish Biol. *10*, 121-173.

Lewis, J.L., Bonner, J., Modrell, M., Ragland, J.W., Moon, R.T., Dorsky, R.I., and Raible, D.W. (2004). Reiterated Wnt signaling during zebrafish neural crest development. Development *131*, 1299-1308.

Liem, K.F., Jr., Tremml, G., Roelink, H., and Jessell, T.M. (1995). Dorsal differentiation of neural plate cells induced by BMP-mediated signals from epidermal ectoderm. Cell *82*, 969-979.

Mesman, S., von Oerthel, L., and Smidt, M.P. (2014). Mesodiencephalic dopaminergic neuronal differentiation does not involve GLI2A-mediated SHH-signaling and is under the direct influence of canonical WNT signaling. PLoS One *9*, e97926.

Moury, J.D. and Jacobson, A.G. (1990). The origins of neural crest cells in the axolotl. Dev. Biol. *141*, 243-253.

Nguyen, V.H., Schmid, B., Trout, J., Connors, S.A., Ekker, M., and Mullins, M.C. (1998). Ventral and lateral regions of the zebrafish gastrula, including the neural crest progenitors, are established by a bmp2b/swirlpathway of genes. Dev. Biol. *199*, 93-110.

Okumura, F., Fujiki, Y., Oki, N., Osaki, K., Nishikimi, A., Fukui, Y., Nakatsukasa, K., and Kamura, T. (2020). Cul5-type ubiquitin ligase KLHDC1 contributes to the elimination of truncated SELENOS produced by failed UGA/Sec decoding. iScience *23*, 100970.

Park, H.C., Mehta, A., Richardson, J.S., and Appel, B. (2002). olig2 is required for zebrafish primary motor neuron and oligodendrocyte development. Dev. Biol. *248*, 356-368.

Polymeropoulos, M.H., Higgins, J.J., Golbe, L.I., Johnson, W.G., Ide, S.E., Di Iorio, G., Sanges, G., Stenroos, E., Pho, L.T., Schaffer, A.A., et al. (1996). Mapping of a gene for Parkinson's disease to chromosome 4q21-q23. Science *274*, 1197-1199.

Polymeropoulos, M.H., Lavedan, C., Leroy, E., Ide, S.E., Dehejia, A., Dutra, A., Pike, B., Root, H., Rubenstein, J., Boyer, R., et al. (1997). Mutation in the α-synuclein gene identified in families with Parkinson's disease. Science *276*, 2045-2047.

Russek-Blum, N., Gutnick, A., Nabel-Rosen, H., Blechman, J., Staudt, N., Dorsky, R.I., Houart, C., and Levkowitz, G. (2008). Dopaminergic neuronal cluster size is determined during early forebrain patterning. Development *135*, 3401-3413.

Ryu, S.W., Chae, S.K., Lee, K.J., and Kim, E. (1999). Identification and characterization of human Fas associated factor 1, hFAF1. Biochem. Biophys. Res. Commun. *262*, 388-394.

Sherman, B.T. and Lempicki, R.A. (2009). Systematic and integrative analysis of large gene lists using DAVID bioinformatics resources. Nat. Protoc. *4*, 44.

Simeone, A., Di Salvio, M., Di Giovannantonio, L.G., Acampora, D., Omodei, D., and Tomasetti, C. (2011). The role of otx2 in adult mesencephalic–diencephalic dopaminergic neurons. Mol. Neurobiol. *43*, 107-113.

Smeets, W.J.A.J. and Reiner, A. (1994). Catecholamines in the CNS of vertebrates: current concepts of evolution and functional significance. In Phylogeny and Development of Catecholamine Systems in the CNS of Vertebrates, W.J.A.J. Smeets and A. Reiner, eds. (Cambridge: Cambridge University Press), pp. 463-481.

Stigloher, C., Ninkovic, J., Laplante, M., Geling, A., Tannhäuser, B., Topp, S., Kikuta, H., Becker, T.S., Houart, C., and Bally-Cuif, L. (2006). Segregation of telencephalic and eye-field identities inside the zebrafish forebrain territory is controlled by Rx3. Development *133*, 2925-2935.

Sul, J.W., Park, M.Y., Shin, J.H., Kim, Y.R., Yoo, S.E., Kong, Y.Y., Kwon, K.S., Lee, Y.H., and Kim, E. (2013). Accumulation of the parkin substrate, FAF1, plays a key role in the dopaminergic neurodegeneration. Hum. Mol. Genet. *22*, 1558-1573.

TeSlaa, J.J., Keller, A.N., Nyholm, M.K., and Grinblat, Y. (2013). Zebrafish Zic2a and Zic2b regulate neural crest and craniofacial development. Dev. Biol. *380*, 73-86.

Tofaris, G.K. and Spillantini, M.G. (2007). Physiological and pathological properties of α-synuclein. Cell. Mol. Life Sci. *64*, 2194-2201.

Trapnell, C., Pachter, L., and Salzberg, S.L. (2009). TopHat: discovering splice junctions with RNA-Seq. Bioinformatics *25*, 1105-1111.

Villanueva, S., Glavic, A., Ruiz, P., and Mayor, R. (2002). Posteriorization by FGF, Wnt, and retinoic acid is required for neural crest induction. Dev. Biol. *241*, 289-301.

Wakabayashi, K., Tanji, K., Mori, F., and Takahashi, H. (2007). The Lewy body in Parkinson's disease: molecules implicated in the formation and degradation of α-synuclein aggregates. Neuropathology *27*, 494-506.

Werner, A., Iwasaki, S., McGourty, C.A., Medina-Ruiz, S., Teerikorpi, N., Fedrigo, I., Ingolia, N.T., and Rape, M. (2015). Cell-fate determination by ubiquitin-dependent regulation of translation. Nature *525*, 523-527.

Yu, C., Kim, B.S., and Kim, E. (2016). FAF1 mediates regulated necrosis through PARP1 activation upon oxidative stress leading to dopaminergic neurodegeneration. Cell Death Differ. *23*, 1873-1885.